Biophysical Journal Volume 67 August 1994 521–529

Computer Simulation of a Model Network for the Erythrocyte Cytoskeleton

David H. Boal
Department of Physics, Simon Fraser University, Burnaby, British Columbia V5A 1S6, Canada

ABSTRACT The geometry and mechanical properties of the human erythrocyte membrane cytoskeleton are investigated by a computer simulation in which the cytoskeleton is represented by a network of polymer chains. Four elastic moduli as well as the area and thickness are predicted for the chain network as a function of temperature and the number of segments in each chain. Comparisons are made with mean field arguments to examine the importance of steric interactions in determining network properties. Applied to the red blood cell, the simulation predicts that in the bilayer plane the membrane cytoskeleton has a shear modulus of $10 \pm 2 \times 10^{-6}$ J/m^2 and an areal compression modulus of $17 \pm 2 \times 10^{-6}$ J/m^2. The volume compression modulus and the transverse Young's modulus of the cytoskeleton are predicted to be $1.2 \pm 0.1 \times 10^3$ J/m^3 and $2.0 \pm 0.1 \times 10^3$ J/m^3, respectively. Elements of the cytoskeleton are predicted to have a mean displacement from the bilayer plane of 15 nm. The simulation agrees with some, but not all, of the shear modulus measurements. The other predicted moduli have not been measured.

INTRODUCTION

The human red blood cell (RBC) has extraordinary elasticity and fatigue resistance (Steck, 1989). During its 120-day lifetime, an RBC squeezes through capillaries roughly ⅓ of its equilibrium diameter on the order of 10^5 times. The two-component structure of the RBC plasma membrane, a fluid lipid bilayer coupled to a network of spectrin protein, gives rise to its intriguing mechanical properties. It was proposed some years ago that the lipid bilayer is primarily responsible for the membrane's resistance to compression, and the spectrin network provides the resistance to shear (Evans, 1973; Skalak et al., 1973; Stokke et al., 1986; Elgsaeter and Mikkelsen, 1991). Computer simulation has verified that, as the spectrin density decreases, the compression modulus K_A of the bilayer and shear modulus μ of the spectrin network decouple and their ratio changes by several orders of magnitude (Boal et al., 1992).

The RBC membrane cytoskeletal network is known to be composed of spectrin tetramers linked together at approximately sixfold coordinate junction complexes yielding a network of mainly triangular connectivity (Steck, 1989). The contour length l_c of the spectrin tetramer is approximately 200 nm, and the average distance between the junction complexes is about 75 nm (Steck, 1989; Liu et al., 1987; Vertessy and Steck, 1989; McGough and Josephs, 1990). Thus, the zero-pressure equilibrium area (projected on the bilayer plane) of the network is approximately ⅓ of its fully stretched area. Several measurements have been made of the network's shear modulus, with some measurements yielding values in the $(6–9) \times 10^{-6}$ J/m^2 range and others yielding less than 10^{-6} J/m^2 (Waugh and Evans, 1979; Hochmuth, 1987; Engelhardt and Sackmann, 1988; Zilker et al., 1992; Peterson et al., 1992).

Some simple arguments from polymer physics can be used to interpret the equilibrium size and elastic moduli of the spectrin network. A single freely jointed polymer chain has an end-to-end distance r_{ee} in coordinate space, which is considerably less than its contour length l_c. This characteristic arises from entropic considerations because there are far fewer configurations in which the chain is fully stretched (large r_{ee}) than there are for convoluted chains (small r_{ee}). Hence, a single chain resists stretching, and a network of chains should have non-zero elastic moduli. Mean field estimates based on the elastic properties of a single polymer chain yield correct order-of-magnitude estimates for the shear modulus of a chain network.

A network of objects, such as springs or chains, can have very different properties than the objects do in isolation. Consider, for example, a single spring with spring constant k and zero equilibrium length. At finite temperature, the mean fluctuation in the spring length is $\langle x \rangle = (2/\pi\beta k)^{1/2}$, where $\beta = 1/k_B T$ with T the temperature and k_B Boltzmann's constant. Suppose we construct a two-dimensional triangular network of these springs, with each spring joined to a sixfold coordinate junction. If each spring in the network has the same $\langle x \rangle$ as an isolated spring, then we expect the area per junction to be $3^{1/2}/(\pi\beta k) = 0.55/\beta k$. In fact, two-dimensional networks in which the springs are not allowed to intersect each other have an area per junction vertex that is about half of this value, $0.33/\beta k$ (Boal et al., 1993). Worse still, if the steric interaction between the springs is ignored, the network collapses and the area per vertex vanishes as the number of junctions increases. Collapse also occurs for membranes embedded in three dimensions (Kantor and Nelson, 1987a; Kantor and Nelson, 1987b).

We conclude from this example that:

(i) Networks can have very different properties than their individual components do in isolation.

Received for publication 14 June 1993 and in final form 13 May 1994.

Address reprint requests to David H. Boal, Department of Physics, Simon Fraser University, Burnaby, British Columbia, Canada V5A 1S6. Tel.: 604-291-5765; Fax: 604-291-3592; E-mail: boal@sfu.ca.

0006-3495/94/08/521/09 $2.00

(ii) The steric interaction between the elements in a network can strongly affect the network's properties.

In other words, calculations of cytoskeleton properties that are based on single chains or springs, and ignore the correlations that are present in a network, are best regarded as order of magnitude estimates only. In some cases, such numerical estimates can be accurate to within a factor of two, whereas in other cases they might not be able to reproduce the essential physics at all. However, to predict erythrocyte cytoskeleton properties at the 10–20% accuracy level requires a more detailed approach than mean field theory.

Here, we report a detailed computer simulation of a polymer chain network that allows us to make accurate predictions of the network's elastic moduli and also to investigate the network's spatial geometry. The paper is organized as follows. The simulation model and techniques are presented in the next section of the paper. The geometrical predictions of the model network are then discussed, including the predicted network thickness, and this is followed by a presentation of the network's elastic properties as a function of the number of segments in each chain. Although the model results are completely general, the erythrocyte membrane cytoskeleton is the motivation for the model's development. Hence, a section of the paper is devoted to the specific predictions of the model for erythrocyte properties. Currently, measurements are available for only two of the model's predictions for the RBC membrane cytoskeleton; the remaining predictions await further experiments. The paper concludes with comparisons of the model against mean field and other arguments to isolate the dependence of the network properties on steric interactions, specifically, the interactions within and between spectrin, and between the cytoskeleton and the lipid bilayer.

SIMULATION MODEL AND TECHNIQUES

A given spectrin tetramer is represented in the simulation by a chain of n_{seg} segments, each segment composed of a straight flexible tether ending at hard beads of diameter a. The individual tethers have a minimum end-to-end distance of a, as determined by the hard-core radius of the beads. If the tethers are forbidden from passing through each other, then their maximum length must be less than $2^{1/2}a$. In the simulation, we use a maximum length of $1.9^{1/2}a$, because the beads move in finite steps and could jump across a tether of length $2^{1/2}a$. The average end-to-end distance *along* a single chain (defined as the contour length l_c) is then

$$l_c = 1.2n_{seg}a. \quad (1)$$

Simulations of other chain networks have been used previously in the study of membrane flatness (Abraham and Goulian, 1992; Petsche and Grest, 1993).

The midpoints of each chain are constrained to move only in the computational xy plane that represents the lipid bilayer, similar to the way in which spectrin is attached to the bilayer by ankyrin (see Steck, 1989). Given the bilayer's resistance to bending, it is expected that the bilayer is flat on the length scale of the simulation (0.3 μm). The ends of the chains are linked at junction vertices to form a triangular network, in the same way as the spectrin tetramers are joined at their ends by actin and band 4.1 proteins. The sixfold junctions are not attached to the xy plane. A sample configuration for $n_{seg} = 20$ is shown in Fig. 1, in which only the positions of the tethers have been drawn. Fig. 1 *a* is a face view of the network, looking from the z axis towards the computational xy plane representing the lipid bilayer. Fig. 1 *b* is a side view of the same configuration, in which the xy plane is viewed edge-on. Positive z is towards the interior of the cell. The shading is such that segments that are further away from the viewer appear darker.

The simulation uses the Monte Carlo technique. Each bead on the chain is allowed to move freely on the positive z side of the xy plane, subject only to the constraints imposed by the tether length and hard bead interactions. The maximum change in a given bead's Cartesian coordinate during a Monte Carlo move is $\pm 0.1a$. The network is subject to periodic boundary conditions (PBCs) in the x and y directions, with repeat distances of L_x and L_y, respectively. The black background area in Fig. 1 *a* indicates the size of the PBC box. The simulation is performed at zero pressure, in which L_x and L_y are allowed to fluctuate independently (Wood, 1968; Hansen and McDonald, 1986). A *sweep* across the network involves one trial move on each of the bead positions, and one trial rescaling of the box lengths. The change in the box rescaling is accepted according to a Boltzmann weight $\exp[N_b \ln(1 + \Delta A_{xy}/A_{xy})]$, where N_b is the total number of segment joints (i.e., beads) in the network, A_{xy} is the PBC box area L_xL_y, and ΔA_{xy} is the difference in A_{xy} associated with the rescaling move. Subscripts are included on A_{xy} to distinguish this area from A, which is used in later sections as the area per junction vertex. That is, $A = A_{xy}/N_j$, where N_j is the number of junction vertices. If there are N_j sixfold junction vertices within the PBC box, then $N_b = N_j(3n_{seg} - 2)$.

In the simulations, 16 junction vertices are used, and n_{seg} is investigated over the range 4–30. Separate simulations are performed at $n_{seg} = 6$ with 16 and 36 junction vertices to check for finite system size effects. The elastic constants obtained with $N_j = 16$ and 36 are found to be identical within statistical errors. The Monte Carlo technique generates a sequence of configurations that is available for constructing ensemble averages. In practice, only 300–500 configurations are used in the construction of averages for $4 \leq n_{seg} \leq 20$, each configuration separated by $\tau = 100N_b$ sweeps, so that the correlation between successive configurations is reduced. Further, the system is allowed to relax for 10τ before sample collection begins. The entire simulation took 1 year to execute on a 40 MHz MIPS R3000 processor.

The in-plane elastic moduli K_A and μ are determined from the fluctuations in the values of L_x and L_y using a method that has been described previously (Boal et al., 1992) and that is briefly reviewed here. The projections of the bead positions on the xy plane can be described in the continuum limit by

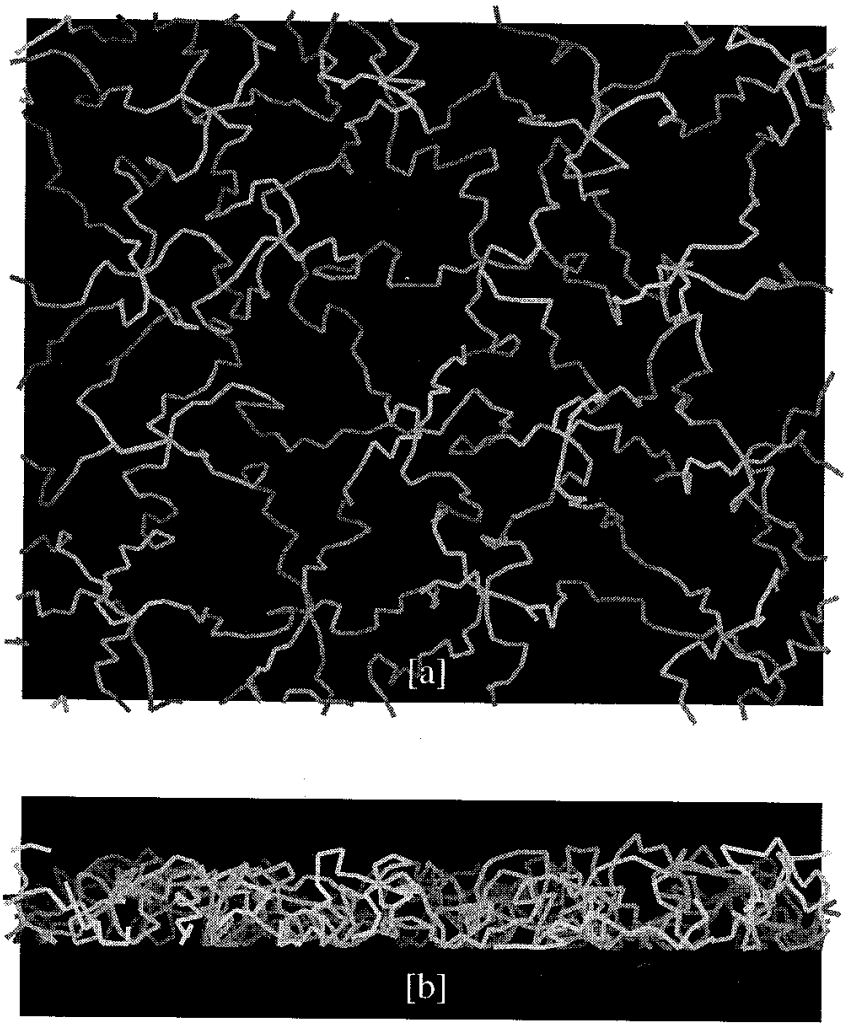

FIGURE 1 Sample configuration for a network at zero pressure with $n_{seg} = 20$ elements per chain. The 16 junction vertices are sixfold coordinate. (*a*) View is towards the computational bilayer (*xy* plane) as seen from the "cytoplasmic" side. The size of the periodic boundary condition box is indicated in black. (*b*) View along the *xy* plane. No chain elements are allowed to pass below $z = 0$. For clarity, the beads have been omitted from the drawing and only the tethers are displayed.

two lateral displacement fields u_1 and u_2, which are functions of the reference coordinate system (x_1, x_2) of the *xy* plane. In terms of the strain tensor

$$u_{ij} = \frac{\partial u_i/\partial x_j + \partial u_j/\partial x_i}{2}, \tag{2}$$

the elastic energy can be written in the continuum limit as (Landau and Lifshitz, 1959)

$$H_{el} = \int d^2x \left\{ \frac{K_A(u_{11} + u_{22})^2}{2} + \mu \left[\frac{(u_{11} - u_{22})^2}{2} + 2u_{12}^2 \right] \right\}. \tag{3}$$

Using Eq. 3, the in-plane compression modulus, for example, can be expressed as

$$\beta K_A = \frac{\langle A_{xy} \rangle}{\langle A_{xy}^2 \rangle - \langle A_{xy} \rangle^2}. \tag{4}$$

Two independent determinations of the in-plane Young's moduli Y_x and Y_y are obtained from fluctuations of the rectangle length in the *x* and *y* directions, respectively:

$$\beta Y_x = [\langle A_{xy} \rangle (\langle L_x^2 \rangle / \langle L_x \rangle^2 - 1)]^{-1} \tag{5a}$$

$$\beta Y_y = [\langle A_{xy} \rangle (\langle L_y^2 \rangle / \langle L_y \rangle^2 - 1)]^{-1}. \tag{5b}$$

We define the in-plane Young's modulus $Y_\parallel$ as the average of Y_x and Y_y. The shear modulus is then obtained from

$$\mu = Y_\parallel K_A / (4K_A - Y_\parallel). \tag{6}$$

The thickness *t* of the membrane in the direction perpendicular to the *xy* (bilayer) plane can be defined by

$$t \equiv \langle z \rangle, \tag{7}$$

where $\langle z \rangle$ is the average height of the bead positions above

the xy (bilayer) plane in a given configuration. Analogous with Eq. 4, the volume compression modulus can be obtained from

$$\beta K_V = \langle V \rangle / (\langle V^2 \rangle - \langle V \rangle^2), \tag{8}$$

where we use $V = A_{xy}t$. Finally, the Young's modulus $Y_\perp$ in the direction normal to the xy (bilayer) plane can be extracted from the fluctuations in t:

$$\beta Y_\perp = [\langle t \rangle / (\langle t^2 \rangle - \langle t \rangle^2)] / \langle A_{xy} \rangle. \tag{9}$$

Note that βK_A and $\beta\mu$ have units of $[length]^{-2}$, whereas βK_V and $\beta Y_\perp$ have units of $[length]^{-3}$.

NETWORK GEOMETRY

We now turn to results from the simulation. As discussed in the introduction, entropic considerations result in a single chain having an end-to-end displacement r_{ee} that is smaller than its contour length l_c. For an ideal chain (self-intersections allowed) with n_{seg} segments each of length b, $\langle r_{ee}/b \rangle$ grows like $n_{seg}^{1/2}$, whereas l_c/b is equal to n_{seg}. Thus, $\langle r_{ee} \rangle / l_c$ scales like $n_{seg}^{-1/2}$; that is, the end-to-end displacement decreases relative to the contour length as the number of chain segments increases. As will be discussed in a later section, even when chain self-avoidance is included, $\langle r_{ee} \rangle / l_c$ still decreases with n_{seg}, although not as rapidly as in the ideal chain case.

We expect the same general type of behavior for a network of chains: even though the network area increases with n_{seg}, relatively speaking the network shrinks compared with its fully stretched area. We define A as the in-plane area per junction vertex ($A = A_{xy}/N_j$). An approximate fit to the ensemble average of the area A, which is generated by the simulation, yields

$$\langle A/a^2 \rangle = 2.1 n_{seg}^{5/4}. \tag{10}$$

The network has a finite displacement from the computational xy plane binding the chain midpoints. One measure of the network thickness is the mean displacement of the chain beads from the binding plane, which we define as $t \equiv \langle z \rangle$ for a single network configuration. The ensemble average found from the simulation can be approximately fit by

$$\langle t/a \rangle = 0.17 n_{seg}^{4/5}. \tag{11}$$

This shows that both the area and thickness increase with the number of segments in the chains. The product $\langle A \rangle \langle t \rangle$ scales roughly as n_{seg}^2. This scaling behavior indicates that the network is not densely packed, in that a closely packed network of beads would show $\langle A \rangle \langle t \rangle$ scales like n_{seg}^1.

To facilitate a comparison with the "stretched" network, we define a reference area A_c as the area per junction vertex that the network would have if it were composed of straight chains of length l_c. Then $A_c = (3^{1/2}/2) l_c^2$ (where $l_c = 1.2 n_{seg} a$ in the simulation) and A_c scales like n_{seg}^2. Eq. 10 indicates that $\langle A/a^2 \rangle$ scales like $n_{seg}^{5/4}$, showing that $\langle A \rangle$ does increase with the number of segments. Hence, $\langle A \rangle / A_c$ scales like $n_{seg}^{-3/4}$, showing that A decreases relative to the contour area as n_{seg} increases. To make a comparison with the membrane cytoskeleton easier, Fig. 2 shows the ratio of A_c to $\langle A \rangle$ for the network at zero pressure. We find that $A_c/\langle A \rangle$ can be fitted by $0.6 n_{seg}^{0.75}$, which is the solid line in Fig. 2. We return to the implications of this scaling behavior in a later section of the paper.

Because the network's mean in-plane area is significantly less than its stretched area, the network is displaced from the bilayer plane. Eq. 11 indicates that the thickness of the chain network increases with the number of chain segments, scaling as $n_{seg}^{4/5}$. However, t does not increase as fast as the contour length l_c so that $\langle t \rangle / l_c$ decreases slowly with increasing n_{seg} or, equivalently, $l_c/\langle t \rangle$ increases with n_{seg}, as shown in Fig. 2.

Fig. 2 deals with the behavior of the mean values of the network area and thickness. We find that the fluctuations in these quantities around their mean values are not large. In Fig. 3, we show a scatter plot of the values of A and t for the particular choice of $n_{seg} = 20$. What is shown are the values of $(A/\langle A \rangle) - 1$ and $(t/\langle t \rangle) - 1$ for each configuration used in the ensemble average. As expected, the points are clustered near the origin and show that few configurations in the sample fluctuate more than 15% away from the mean. What is more noticeable is that there is a correlation between A and t running from the upper left to the lower right part of the figure. This tells us that the "volume per junction vertex" of the system At does not fluctuate strongly over the ensemble. That is, if the area of the network is larger than average, then the thickness tends to be smaller than average. The relative constancy of A and t provides a link between several of the elastic constants, as is shown in the next section.

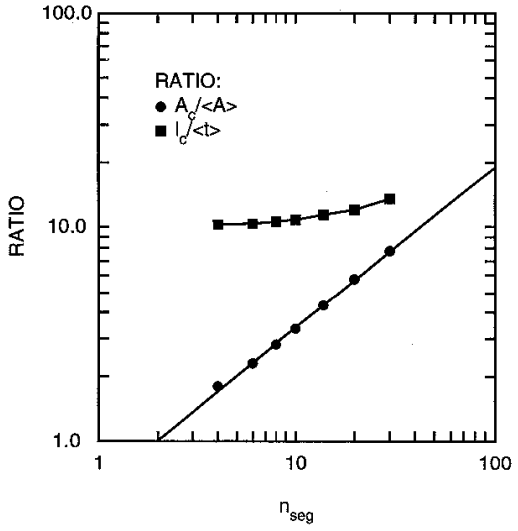

FIGURE 2 Ratios of stretched to equilibrium quantities as a function of segment number n_{seg}. The stretched area per junction vertex A_c is compared with the mean area per junction vertex $\langle A \rangle$, and the contour length l_c is compared with the mean displacement $\langle t \rangle$. The solid straight line through the $A_c/\langle A \rangle$ data is the equation $A_c/\langle A \rangle = 0.6 n_{seg}^{0.75}$. Data are obtained with $N_j = 16$.

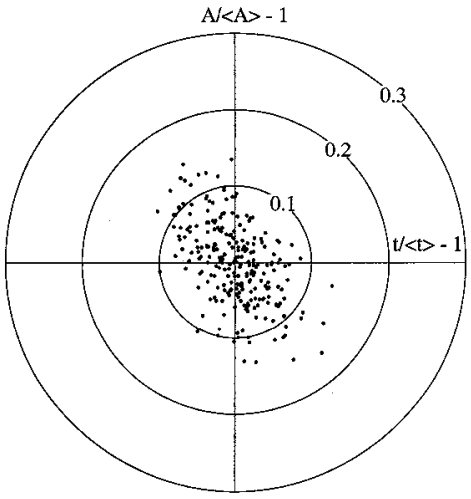

FIGURE 3 Scatter plot of area per junction vertex A and thickness t for $n_{seg} = 20$ configurations. Each point represents a pair of values $(A/\langle A\rangle) - 1$ and $(t/\langle t\rangle) - 1$.

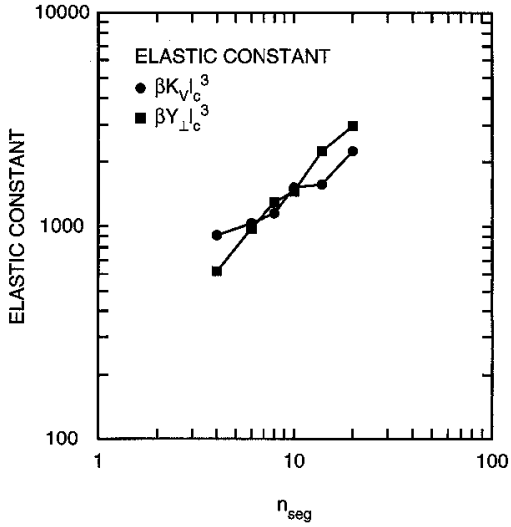

FIGURE 5 Volume compression modulus $\beta K_V l_c^3$ and transverse Young's modulus $\beta Y_\perp l_c^3$ predicted for the chain network as a function of n_{seg}. Data are obtained with $N_j = 16$.

NETWORK ELASTICITY

The elastic moduli K_A, μ, K_V, and $Y_\perp$ and can be obtained from fluctuations in the PBC box size and network thickness as explained in the section on simulation techniques. The values for all four moduli are shown in Figs. 4 and 5 as a function of n_{seg}. Because the moduli are determined from fluctuations, there is a larger statistical uncertainty in their value than there is for $\langle A\rangle$ or $\langle t\rangle$. We estimate the errors for the moduli shown in Figs. 4 and 5 at approximately 10%.

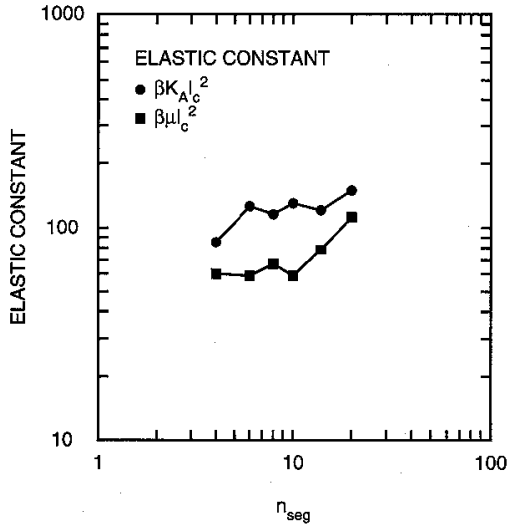

FIGURE 4 In-plane area compression modulus $\beta K_A l_c^2$ and shear modulus $\beta\mu l_c^2$ predicted for the chain network as a function of n_{seg}. Data are obtained with $N_j = 16$.

Results for $n_{seg} = 30$ are not shown because machine time limitations restrict our data set to 60 configurations, and the moduli cannot be extracted from such a small data set.

The quantities plotted in Figs. 4 and 5 are unitless: the moduli have been multiplied by appropriate powers of the inverse temperature β and contour length l_c to render them dimensionless. The resulting quantities are dependent on n_{seg} over the range shown: the reduced in-plane moduli ($\beta K_A l_c^2$ and $\beta\mu l_c^2$) increase only weakly with n_{seg}, whereas the reduced volume moduli ($\beta K_V l_c^3$ and $\beta Y_\perp l_c^3$) rise roughly linearly with n_{seg}. However, the moduli themselves decrease with chain length, because $l_c = 1.2an_{seg}$. Fits to the raw data that go into Fig. 4 show that the in-plane moduli are described approximately as

$$\beta K_A a^2 = 43 n_{seg}^{-1.7} \tag{12}$$

and

$$\beta\mu a^2 = 25 n_{seg}^{-1.7} \tag{13}$$

This gives a ratio of the in-plane compression modulus to the shear modulus of 1.7. The other moduli that are used in the construction of Fig. 5 can be fit by

$$\beta K_V a^3 = 193 n_{seg}^{-2.4} \tag{14}$$

and

$$\beta Y_\perp a^3 = 87 n_{seg}^{-2.0}. \tag{15}$$

The decrease in the moduli with n_{seg} is no surprise, because the network is more open (as measured in bead diameter a) and less resistant to stress as n_{seg} increases.

The temperature dependence of the moduli is also contained in Figs. 4 and 5. At fixed chain length, all of the moduli

are found to increase linearly with temperature. This behavior arises because the chains in the simulation have no explicit energy scale because they have only hard core interactions. Thus, the expressions for the elastic moduli in Eqs. 4, 5, 8, and 9 have no temperature dependence on their right-hand sides. This tells us that any elastic modulus divided by k_BT is constant at fixed n_{seg} in this simulation, so that the elastic moduli increase linearly with temperature.

The relatively small fluctuations in A and t indicated by Fig. 3 allow one to find approximate relationships between the compression moduli. For example, if we use $V \approx A_{xy}\langle t\rangle$, then Eqs. 4, 8, and 9 yield

$$\beta K_A/t \approx \beta K_V \tag{16}$$

and

$$\beta Y_\perp \approx \beta K_V. \tag{17}$$

Let us take the results from around $n_{seg} = 20$ as an example. From Figs. 2 and 4, we have $l_c/\langle t\rangle \approx 12$ and $\beta K_A l_c^2 \approx 150$. Eq. 16 then predicts $\beta K_V l_c^3 \approx 1800$, which can be compared with a value of about 2400 from Fig. 5. Similarly, one can see directly from Fig. 5 that Eq. 17 is approximately satisfied. Hence, the small fluctuations in the network geometry yield relationships among the elastic constants that are accurate to about 30%.

APPLICATION TO ERYTHROCYTES

To apply the general network results from the previous sections to the erythrocyte membrane cytoskeleton, we have to set the temperature and length scale, because the simulation predicts the values of reduced quantities such as $\beta\mu l_c^2$. We choose $T = 300$ K to set the temperature scale and use the ratio $A_c/\langle A\rangle$ to set the length scale of the simulation. Experimentally, $A_c/\langle A\rangle$ is measured to be approximately 7, which corresponds to $n_{seg} = 26 \pm 1$ on Fig. 2 (Steck, 1989; Liu et al., 1987; Vertessy and Steck, 1989; McGough and Josephs, 1990). The spectrin tetramer has a measured contour length l_c of 200 nm, which means that the computational spectrin in our simulation behaves like a chain with 26 segments between the sixfold junctions, each segment of length 8 nm (or $a = 6.4$ nm). This result is in the range of values for the spectrin persistence length of ≈10 nm obtained in recent experiments on RBC skeletons in salt solution (Svoboda et al., 1992; see also Stokke et al., 1985).

With T, n_{seg}, and l_c fixed, the thickness and elastic moduli can be extracted from Figs. 2, 4, and 5. For n_{seg} in the 25–27 range, we find $l_c/\langle t\rangle = 13.1 \pm 0.1$ on Fig. 2. If l_c is 200 nm, this corresponds to a thickness of $\langle t\rangle = 15$ nm. Currently, no data are available against which the thickness prediction can be compared.

The range of values for the in-plane moduli around $n_{seg} = 26$ is about 0.16–0.18 for $\beta K_A a^2$ and 0.09–0.11 for $\beta\mu a^2$, according to Eqs. 12, 13, and Fig. 4. Using $a = 6.4$ nm, the simulation predicts $K_A = 17 \pm 2 \times 10^{-6}$ J/m^2 and $\mu = 10 \pm 2 \times 10^{-6}$ J/m^2 at $T = 300$ K. Currently, only the shear modulus has been measured. In one type of experiment, the deformation of an RBC subject to a known stress induced by micromechanical manipulation is visually recorded, from which a shear modulus of 6–9 $\times 10^{-6}$ J/m^2 is extracted (Waugh and Evans, 1979; Hochmuth, 1987). A related experiment using deformations in high frequency electric fields yields $6 \pm 1 \times 10^{-6}$ J/m^2 (Engelhardt and Sackmann, 1988). In other experiments based on flicker spectroscopy, the surface fluctuations of the cell at wavelengths on the order of microns (Zilker et al., 1992) and longer (Peterson et al., 1992) have been shown to be consistent with those of a pure fluid membrane ($\mu = 0$). Thus, the predicted shear modulus is in agreement with the measured values of the micromechanical and the high frequency deformation experiments at the one or two standard deviation level.

From Eqs. 14, 15, and Fig. 5, the simulation predicts $\beta K_V a^3$ has a value of $7.8 \pm 0.8 \times 10^{-2}$, corresponding to $K_V = 1.2 \pm 0.1 \times 10^3$ J/m^3. A measurement of this compression modulus is currently being performed (E. Evans, personal communication). The transverse Young's modulus $Y_\perp$ can also be obtained from Fig. 5, and is predicted to be $\beta Y_\perp a^3 = 0.13 \pm 0.01$, or $Y_\perp = 2.0 \pm 0.1 \times 10^3$ J/m^3. Although no data are currently available for $Y_\perp$, it will be measured along with K_V.

The elastic moduli increase linearly with temperature in the simulation, according to Figs. 4 and 5. Over the range 5–35°C, the moduli should increase by 10% if n_{seg} and l_c are constant. In fact, the moduli decrease by about 20% in this temperature range (Waugh and Evans, 1979; Engelhardt and Sackmann, 1988). Within the context of the model, this behavior would indicate that interactions among chain elements are changing the value of n_{seg} slowly with temperature. Discussions of chain interactions can be found elsewhere (Stokke et al., 1986; McGough and Josephs, 1990).

STERIC INTERACTIONS IN THE NETWORK

The properties of the simulation have simple origins: entropy and steric interactions. The simulation contains no explicit energy scale in the sense of bending resistance or force constants associated with chemical bonds. The entropy of the chains manifests itself in the reduced area of the network compared with its contour area and in the elastic moduli.

In this section, we examine the importance of the steric interactions: for example, the interaction between chains or between the chains and the computational bilayer. Our method is to present simplified models that allow us to isolate and evaluate a given component of the simulation. Each of these simple models can be used to determine some, but not all, of the network's properties. These models have few parameters and make few predictions that can be tested systematically in the way that the simulation can. However, by determining whether the physics of these models is present in the simulation, we can evaluate the importance of the models themselves.

The simulation is not described by ideal random walks

Consider the properties of a single ideal (i.e., not self-avoiding) chain of n_{seg} segments each with length b. The single chain has an end-to-end distance of $\langle r_{ee}^2/b^2\rangle^{1/2} = n_{seg}^{1/2}$. Suppose that we construct a triangular network of such chains, linked together at sixfold vertices as we have done with our simulation. The ideal chain has a gaussian distribution of end-to-end lengths and can be viewed as an entropic spring. A two-dimensional network of ideal springs (ones that can pass through each other) has been shown to collapse at zero pressure (Boal et al., 1993). Hence, the simulation is not described by ideal chains, and the interaction between chains is important.

If the springs cannot pass through each other, the network is stable (Boal et al., 1993). Hence, another test model for the simulation might involve a network of chains that can intersect themselves, but not each other (see, for example, Kozlov and Markin, 1987). If the average properties of a chain in this network are the same as those of the isolated ideal chains, then the area of the network should scale like n_{seg}^1 because $\langle r_{ee}/b\rangle$ scales like $n_{seg}^{1/2}$ for an ideal chain. This is not what we observe: the simulation shows $\langle A\rangle$ scales like $n_{seg}^{5/4}$. We conclude that the steric interaction between elements of the same chain and between elements of different chains are *both* required to reproduce the simulation.

Self-avoiding chains show the correct scaling behavior

The end-to-end distance of an ideal chain scales like $n_{seg}^{1/2}$. In contrast, a self-avoiding chain scales like $\langle r_{ee}^2/b^2\rangle^{1/2} \approx n_{seg}^{3/(2+d)}$, where d is the dimension of the space in which the chains move (Flory, 1971). Hence, a network of self-avoiding chains free to move in three dimensions should obey $A_c/\langle A\rangle \approx n_{seg}^{0.8}$. In Fig. 2, $A_c/\langle A\rangle$ scales like $n_{seg}^{0.75}$, which is consistent with the self-avoiding chain prediction.

Suppose we construct a model network in which the end-to-end displacement of any chain in the network is assumed to be the same as that of a single self-avoiding chain in isolation. How well does this model network represent the full simulation? For a single bead-and-tether chain with contour length $l_c = n_{seg}b$, we find by simulation that $\langle r_{ee}/b\rangle$ can be fit by

$$\langle r_{ee}/b\rangle = 1.04 n_{seg}^{0.6}. \tag{18}$$

From this relationship, the network of identical self-avoiding chains would have $A_c/\langle A\rangle = 0.92 n_{seg}^{0.8}$. This expression is close to, but not identical to, the expression we find in the full simulation, namely $A_c/\langle A\rangle = 0.6 n_{seg}^{0.75}$. For the RBC, we expect $n_{seg} = 26$, for which the simplified model predicts $A_c/\langle A\rangle = 12.4$ in contrast with the simulation result of $A_c/\langle A\rangle = 6.9$. The difference between these two numbers is a measure of the importance of a chain's interaction with other chains and with the bilayer. We conclude that the self-avoidance of the chains is important, and that a simplified network of identical self-avoiding chains can represent the network's in-plane geometry at the factor-of-two level. Of course, we need more than the single chain scaling relations for $\langle r_{ee}\rangle$ to make predictions for the network thickness and elastic moduli perpendicular to the bilayer plane, so the simplified model is of restricted applicability.

The presence of the bilayer plane is important

The steric interactions among chain elements make a crucial contribution to the properties of the simulated network. The other element of the simulation that involves steric effects is the repulsion between the chain elements and the computational xy plane, which represents the bilayer in the simulation. To test the importance of the bilayer plane on the in-plane network elasticity, further test simulations are performed at $n_{seg} = 10$ that can be compared with the general network simulation. Only one value of n_{seg} is chosen for investigation because of machine time limitations. In the first of these test simulations, the bilayer is neglected completely and chain elements can move above and below the computational xy plane. In the second simulation, the midpoints of the chains are confined to the xy plane, but all other chain elements are allowed to move through it. In both simulations, the network is still subject to periodic boundary conditions in the x and y directions. A total of 300 configurations are generated in each simulation.

Complete neglect of the bilayer dramatically affects the network properties. The increased configuration space of the chains results in a significant shrinkage of the network for $n_{seg} = 10$. It is found that $A_c/\langle A\rangle$ increases from 3.3 to 5.3. Similarly, the network becomes floppier because it can relieve stress by folding in the third dimension. Thus, the in-plane compression modulus $\beta K_A l_c^2$ decreases from 131 to 55 and the in-plane shear modulus $\beta\mu l_c^2$ decreases from 59 to 32 when the bilayer is completely removed. These out-of-plane fluctuations should decrease the moduli even further with increasing system size, an effect that has not been investigated here. We conclude that complete removal of the bilayer changes the network properties dramatically.

In a further simulation for $n_{seg} = 10$, any chain element is allowed to pass through the computational xy plane, but the midpoints of the chains are restricted to lie in the xy plane. Only small changes are found in the in-plane quantities. The equilibrium area is found to shrink somewhat without the bilayer repulsion, so that $A_c/\langle A\rangle$ increases from 3.3 to 3.5.The in-plane compression modulus changes from $\beta K_A l_c^2 = 131$ with bilayer repulsion to $\beta K_A l_c^2 = 101$ without. Finally, the shear modulus changes from $\beta\mu l_c^2 = 59$ to $\beta\mu l_c^2 = 63$.

In summary, these results show that attaching the chain midpoints to the flat bilayer stiffens the network substantially compared with a network that is allowed to move freely in the z direction subject only to periodic boundary conditions. The steric interaction of the chains with the bilayer once the network is attached to the bilayer changes the in-plane elastic properties by only 10–20%.

Gaussian chains do not describe the in-plane moduli

Two decades ago, it was proposed (Evans, 1973) that a result from rubber elasticity theory (Flory, 1971) could be used to estimate the cytoskeleton shear modulus. For a system with an area density of chains ρ, the shear modulus is given approximately by

$$\beta\mu = \rho \tag{19}$$

where β is the inverse temperature (Evans, 1973; Stokke et al., 1986; Kozlov and Markin, 1987; Flory, 1971). This expression gives a value for the elastic modulus that is in approximate agreement with experiment. For example, if the average end-to-end distance of a single chain is 75 nm as in the red blood cell, then $\rho = 620\ \mu m^{-2}$ and Eq. 19 predicts $\mu = 2.4 \times 10^{-6}$ J/m^2, at room temperature.

Although this prediction for a red blood cell looks attractive, in fact it is a factor of four lower than the simulation predicts for the same parameters ($10 \pm 2 \times 10^{-6}$ J/m^2). That is, the gaussian chain model underestimates a full model, which includes steric interaction among the chains and between the chains and the bilayer. According to the approximations in Eq. 19, the gaussian chain model predicts that $\beta\mu/\rho$ should equal unity and have no dependence on n_{seg}. However, over the range of n_{seg} investigated in the simulation, Eqs. 10 and 13 yield

$$\beta\mu/\rho \approx 17 n_{seg}^{-0.45} \tag{20}$$

where $\rho = 3/\langle A\rangle$ because there are three chains per junction vertex. Hence, we find that approximations based on gaussian chains do not reproduce the elastic properties of the network simulation, just as we saw previously that gaussian chains do not reproduce the simulation's geometry.

THE CHAIN PERSISTENCE LENGTH

Within the simulation, the erythrocyte membrane cytoskeleton is described as a network of single chains, each with $n_{seg} = 26$ segments. Can 26 be regarded as an accurate value for the effective number of segments in a spectrin tetramer, or is n_{seg} simply a parameter of the simulation that is specific to the self-avoidance algorithm? The self-avoidance algorithm rests upon the bead-and-tether model in which the tether between beads is kept sufficiently short that chain elements cannot pass through each other. This gives a small effective stiffness to the chains, because the interaction between next-nearest neighbor beads prevent a chain from completely doubling back on itself.

To put this more quantitatively, consider the angle between one tether and the next along a single chain. If the tethers are in a straight line in the same direction, we say that the "bond angle" between them is 180°. If the chain doubles back on itself so that two nearest neighbors of a given vertex are coincident, then we say that the bond angle between them is zero. The choice of maximum tether length of $(1.9)^{1/2}a$ tells us that the minimum allowed bond angle in this simulation is approximately 45°. The maximum tether length would have to be equal to $2a$ for the minimum bond angle to be zero.

The fact that the configuration space available in the bead-and-tether model is restricted at small bond angles gives a small effective resistance to bending compared with a chain of thin hard rods. Computationally, the bead-and-tether model is much faster to execute than hard rod models, which is why the bead model is so popular in polymer simulations. We do not have the machine time available to test several different algorithms for self-avoidance on the whole network, so, instead, we make comparisons among different models for single chains.

A single chain obeying the same bead-and-tether model that we have used for the chain network has an end-to-end distance squared given by $\langle r_{ee}^2\rangle^{1/2} = 1.09 b n_{seg}^{3/5}$, where b is the contour length per segment: $b = l_c/n_{seg}$. This shows that the persistence length of the model is close to unity. For comparison, we perform a simulation of chains using another potential drawn from the molecular dynamics simulations of Grest and Kremer (1986) (see also Petsche and Grest, 1993). The Grest/Kremer potential uses a Lennard-Jones-like interaction between chain elements with smooth cut-offs at small and large separations between chain vertices. Applying this model to single chains, we find $\langle r_{ee}^2\rangle^{1/2} = 1.22 b n_{seg}^{3/5}$. These simulation results can be compared with a Monte Carlo simulation of self-avoiding walks on a simple cubic lattice (M. van Prooyen and B. G. Nickel, unpublished data; see Nickel, 1991). The walks show to leading order in n_{seg} that $\langle r_{ee}^2\rangle^{1/2} = 1.108 b n_{seg}^{0.59}$. Clearly, the bead-and-tether model is close to this asymptotic form even at the value of n_{seg} investigated here (n_{seg} = 10–80 for our single chain studies). This indicates that the bead-and-tether model has a persistence length close to the elementary chain link length b.

We can alternatively construct a correlation function for the bond orientations along the chain to determine the chain persistence length. We define $\boldsymbol{n}$ to be a unit vector pointing along a given tether. The correlation is constructed from scalar products of the $\boldsymbol{n}$s at different chain positions, and should decay approximately exponentially as

$$\langle \boldsymbol{n}(0)\boldsymbol{n}(\Delta)\rangle \approx \exp[-\Delta/\xi] \tag{21}$$

where Δ is the number of segments separating the tethers on the chain and ξ is the persistence length. We find that the correlation function for the bond orientations as a function of separation between tethers drops to less than $1/e$ at the nearest neighbor position (i.e., $\Delta = 1$), again indicating a persistence length of b. The correlation function is sufficiently featureless above $b = 2$ that we do not show it explicitly in a figure. Given the behavior of the correlation function, we believe that our ratio of bead diameter to tether length has a persistence length close to b.

From the above, we conclude that to within 10% accuracy, $n_{seg} = 26$ is the effective number of segment lengths in the spectrin tetramer within the context of the simulation. This conclusion would be modified if the *physical* assumptions of

the simulation are incorrect: for example, if both the midpoints and junction vertices of the spectrin are attached to the bilayer plane or if the bilayer is flexible on short length scales.

CONCLUSION

We have constructed a computer simulation of the spectrin network of a human red blood cell in which the elastic properties arise from the entropy of the network. The simulation is a general one in which observables are expressed in terms of temperature and chain contour length. The network consists of chains, each with n_{seg} segments, linked together at sixfold junction vertices. The network shrinks compared with its fully stretched, or contour area, as n_{seg} increases. The reduced elastic moduli $\beta K_A l_c^2$, $\beta \mu l_c^2$, $\beta K_V l_c^3$, and $\beta Y_\perp l_c^3$, all increase with n_{seg}, although none increase faster than n_{seg}^1. The bare elastic moduli such as $\beta K_A a^2$ all decrease with n_{seg}. At fixed n_{seg}, the moduli increase linearly with absolute temperature.

The mean end-to-end distance and the contour length of the spectrin tetramer are used as inputs to extract observables for erythrocytes: within the context of the simulation, each spectrin tetramer of the membrane cytoskeleton behaves like a single self-avoiding chain of 26 ± 1 segments, each segment of length 8 nm. The predicted in-plane shear modulus of the network, $10 \pm 2 \times 10^{-6}$ J/m^2, agrees with the micromechanical and high frequency deformation measurements. We predict the in-plane compression modulus K_A to be $17 \pm 2 \times 10^{-6}$ J/m^2. The bulk compression modulus K_V and transverse Young's modulus $Y_\perp$ are predicted to be $1.2 \pm 0.1 \times 10^3$ J/m^3 and $2.0 \pm 0.1 \times 10^3$ J/m^3, respectively. Finally, the mean displacement of the network from the bilayer plane is predicted to be 15 nm. Most of these predictions await further experiment before they can be tested.

The properties of the simulation are not consistent with simplified models with ideal gaussian springs, either individually or in a network. However, several simplified models using self-avoiding chains are able to reproduce some features of the model at the factor of two level. We conclude from these simplified models that the steric interaction within and between chains, and between chains and the bilayer, are important to the network properties.

The author wishes to thank Evan Evans and Narla Mohandas for many stimulating discussions, particularly for suggesting the volume compression modulus calculation.

This work is supported in part by the Natural Sciences and Engineering Research Council of Canada.

REFERENCES

Abraham, F. F., and M. Goulian. 1992. Diffraction from polymerized membranes: flat *vs.* crumpled. *Europhys. Lett.* 19:293–296.

Boal, D. H., U. Seifert, and J. C. Shillcock. 1993. Negative Poisson ratio in two dimensional networks under tension. *Phys. Rev.* E48:4274–4283.

Boal, D. H., U. Seifert, and A. Zilker. 1992. Dual network model for red blood cell membranes. *Phys. Rev. Lett.* 69:3405–3408.

Elgsaeter, A., and A. Mikkelsen. 1991. Shapes and shape changes in vitro in normal red blood cells. *Biochim. Biophys. Acta.* 1071:273–290.

Engelhardt, J., and E. Sackmann. 1988. On the measurement of shear elastic moduli and viscosities of erythrocyte plasma membranes by transient deformation in high frequency electric fields. *Biophys. J.* 54:495–508.

Evans, E. A. 1973. New membrane concept applied to the analysis of fluid shear- and micropipette-deformed red blood cells. *Biophys. J.* 13: 941–954.

Flory, P. J. 1971. Principles of Polymer Chemistry. Cornell University Press, Ithaca, NY. Chapters X and XI.

Grest, G. S., and K. Kremer. 1986. Molecular dynamics simulation for polymers in the presence of a heat bath. *Phys. Rev.* A33:3628–3631.

Hansen, J. P., and I. R. McDonald. 1986. Theory of Simple Liquids. Oxford University Press, New York.

Hochmuth, R. M. 1987. Properties of Red Blood Cells. *In* Handbook of Bioengineering. R. Skalak and S. Chien, editors. McGraw-Hill, New York. 12.1–12.17.

Kantor, Y., and D. R. Nelson. 1987a. Crumpling transition in polymerized membranes. *Phys. Rev. Lett.* 26:2774–2777.

Kantor, Y., and D. R. Nelson. 1987b. Phase transitions in flexible polymeric surfaces. *Phys. Rev.* A36:4020–4032.

Kozlov, M. M., and V. S. Markin. 1987. Model of red blood cell membrane cytoskeleton: electrical and mechanical properties. *J. Theor. Biol.* 129: 439–452.

Landau, L. D., and E. M. Lifshitz. 1959. Theory of Elasticity. Pergamon, London.

Liu, S.-C., L. H. Derick, and J. Palek. 1987. Visualization of the hexagonal lattice in the erythrocyte membrane cytoskeleton. *J. Cell Biology.* 104: 527–536.

McGough, A. M., and R. Josephs. 1990. On the structure of erythrocyte spectrin in partially expanded membrane skeletons. *Proc. Natl. Acad. Sci. USA.* 87:5208–5212.

Nickel, B. G. 1991. One-parameter recursion model for flexible-chain polymers. *Macromolecules.* 24:1358–1365.

Peterson, M. A., H. Strey, and E. Sackmann. 1992. Theoretical and phase contrast microscope eigenmode analysis of erythrocyte flicker: amplitudes. *J. Phys. II (France).* 2:1273–1285.

Petsche, I. B., and G. S. Grest. 1993. Molecular dynamics simulations of the structure of closed tethered membranes. *J. Phys. I (France).* 1: 1741–1754.

Skalak, R., A. Tozeren, R. P. Zarda, and S. Chien. 1973. Strain energy function of red blood cell membranes. *Biophys. J.* 13:245–264.

Steck, T. L. 1989. Red cell shape. *In* Cell Shape: Determinants, Regulation and Regulatory Role. W. Stein and F. Bronner, editors. Academic Press, New York. 205–246.

Stokke, B. T., A. Mikkelsen, and A. Elgsaeter. 1985. Human erythrocyte spectrin dimer intrinsic viscosity: temperature dependence and implications for the molecular basis of the membrane free energy. *Biochim. Biophys. Acta.* 816:102–110.

Stokke, T., A. Mikkelsen, and A. Elgsaeter. 1986. The human erythrocyte membrane skeleton may be an ionic gel I. Membrane mechanical properties. *Eur. Biophys. J.* 13:203–218.

Svoboda, K., C. F. Schmidt, D. Branton, and S. M. Block. 1992. Conformation and elasticity of the isolated red blood cell membrane skeleton. *Biophys. J.* 63:784–793.

Vertessy, B. G., and T. L. Steck. 1989. Elasticity of the human red cell membrane skeleton, effects of temperature and denaturant. *Biophys. J.* 55:255–262.

Waugh, R., and E. A. Evans. 1979. Thermoelasticity of red blood cell membrane. *Biophys. J.* 26:115–132.

Wood, W. W. 1968. Monte Carlo calculations for hard disks in the isothermal-isobaric ensemble. *J. Chem. Phys.* 48:415–434.

Zilker, A., M. Ziegler, and E. Sackmann. 1992. Spectral analysis of erythrocyte flickering in the 0.3–4 μm^{-1} regime by microinterferometry combined with fast image processing. *Phys. Rev.* A46:7998–8001.